MARBEL
NATIONAL SCIENTIFIC CONFERENCE

Effects of Spatial-Domain Tissue-Specific Smoothing Approaches on Statistical Analysis in Quantitative MRI

A. Jacquemin[1], C. Phillips[1]

[1] GIGA-CRC Human Imaging, University of Liège, Liège, Belgium

Oral Presentation in Scientific Session – MaRBEL 2025

7 February 2025

Contents

From the Study of the Brain to MRI

MARBEL

Anatomical MRI

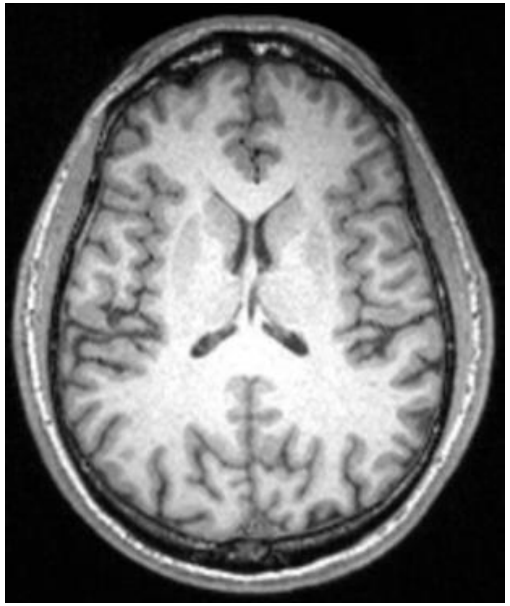

- Gray Matter (GM)
- White Matter (WM)

Quantitative MRI (qMRI)

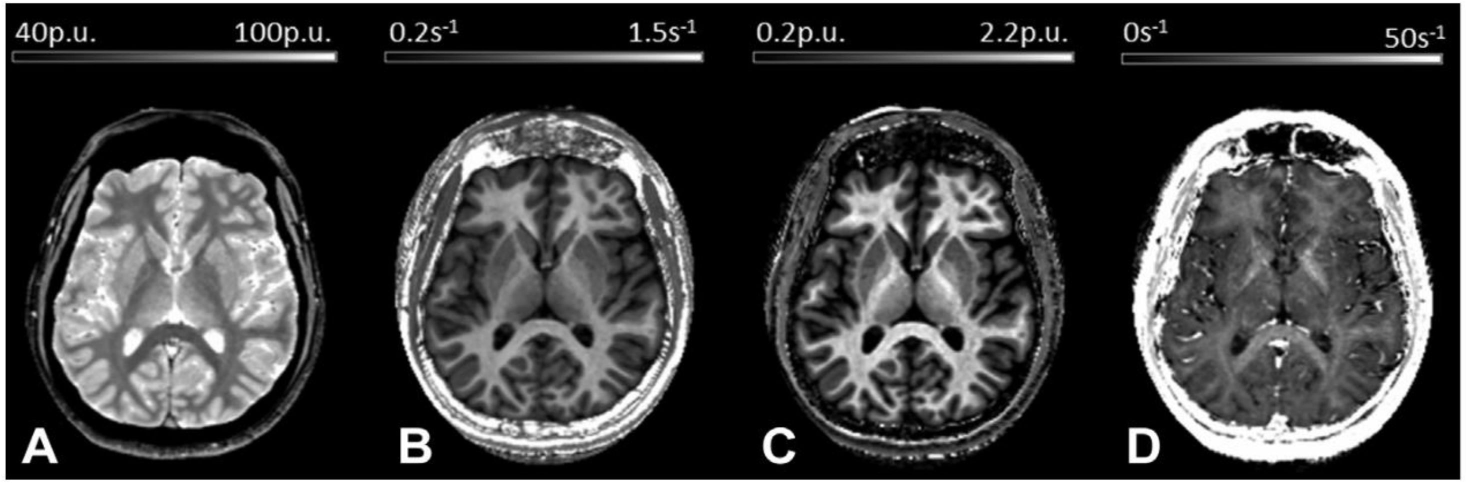

- Quantification of physical properties of brain tissues (GM & WM)
- Interpretability of parameters (PD, R1, MTsat and R2*)
- Standardized units

From the Study of the Brain to Computational Tools

MARBEL

Classical Preprocessing Steps

Segmentation

- Probability of being one tissue or another

Smoothing

- Improving the signal-to-noise ratio
- Reducing inter-subject variability for statistical studies

⇨ Gaussian Smoothing (GS)

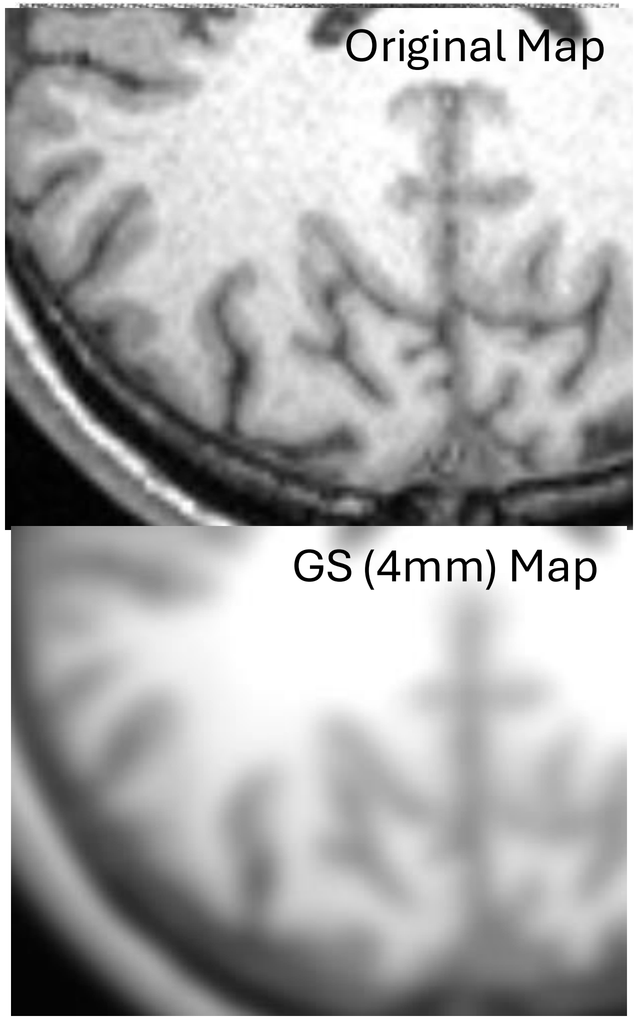

BUT… Introduction of biases near tissue boundaries due to partial volume effects (PVE)

fMRI

qMRI

⇨ Tissue-Specific Smoothing

- Preserving values within each tissue class (reducing PVE)

⇨ Tissue-Weighted Smoothing (TWS)

⇨ Tissue-SPecific smOOthing compeNsated (TSPOON)

Objectives

MARBEL

1. Generalization of TSPOON to GM & WM

2. Comparison of the Effects of TWS vs. generalized TSPOON on qMRI Data

Generalization of TSPOON

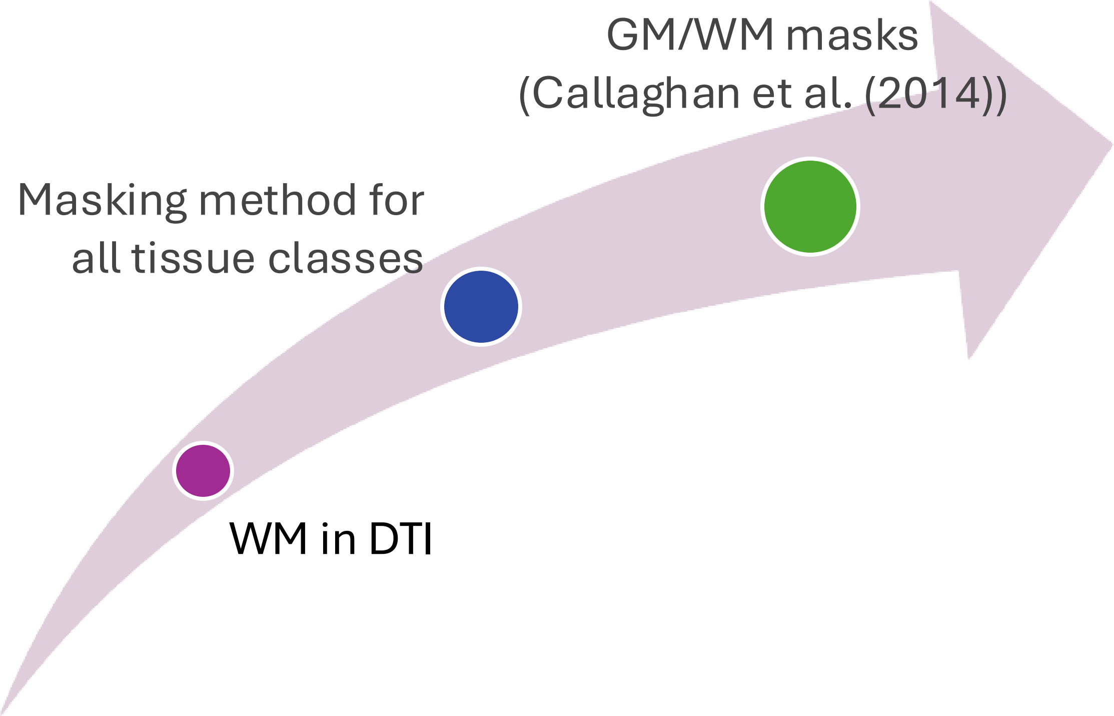

$$signal_{WM}(x) = \frac{g * (M_{WM}.s(\phi))}{g * M_{WM}}$$

Tissue-SPecific smOOthing compeNsated (TSPOON) from Lee et al. (2009)

Generalized TSPOON (GTSPOON)

$$signal_{TC}(x) = \frac{g * (M_{TC}.s(\phi))}{g * M_{TC}} \quad ; \quad g * M_{TC} > 0.05$$

M_{TC} = Winner-Takes-All Tissue masks

Where:

- s(ϕ) = quantitative map warped into standard space
- M_{WM} = white matter mask
- g* = Gaussian isotropic smoothing

Smoothing Approaches

MARBEL

Gaussian Smoothing (GS)

$$G(x,y,z) = \frac{1}{(2\pi)^{3/2}\sigma_x\sigma_y\sigma_z} \exp - \left(\frac{x^2}{2\sigma_x^2} + \frac{y^2}{2\sigma_y^2} + \frac{z^2}{2\sigma_z^2}\right)$$

Tissue-Weighted Smoothing (TWS)

Proposed by Draganski et al. (2011)

$$\text{signal}(x) = \frac{g * (w.s(\phi))}{g * w} \quad ; \quad \text{TPM} > 0.05 \quad \& \quad g * w > 0.05$$

Where w are the modulated tissue-weigths

⇨ Continuous tissue density

Generalized TSPOON (GTSPOON)

Originally proposed by Lee et al. (2009)

$$signal_{TC}(x) = \frac{g * (M_{TC}.s(\phi))}{g * M_{TC}} \quad ; \quad g * M_{TC} > 0.05$$

Where M_{TC} are the binary tissue-specific masks

⇨ Binary tissue density

Comparison Strategies

Reproduction of Callaghan et al.'s aging study (2014)

Dataset of 138 participants (19-75y)
Warped quantitative maps & modulated warped tissue-specific maps

Comparison of SPM's derived from TWS and GTSPOON using statistical approaches
Bland-Altman Plot, Effective Smoothing, Jaccard/Dice/Cohen's kappa Metrics, Threshold Scatter Plot, Cluster-Level Comparison

Differences Induced by Smoothing

Identification of regions significantly affected by the applied smoothing approach (TWS & GTSPOON)

Brain 1D Profile

Analysis of signals extracted along a 1D profile
Signals: original, smoothed using TWS & smoothed using GTSPOON

SPM-based Results

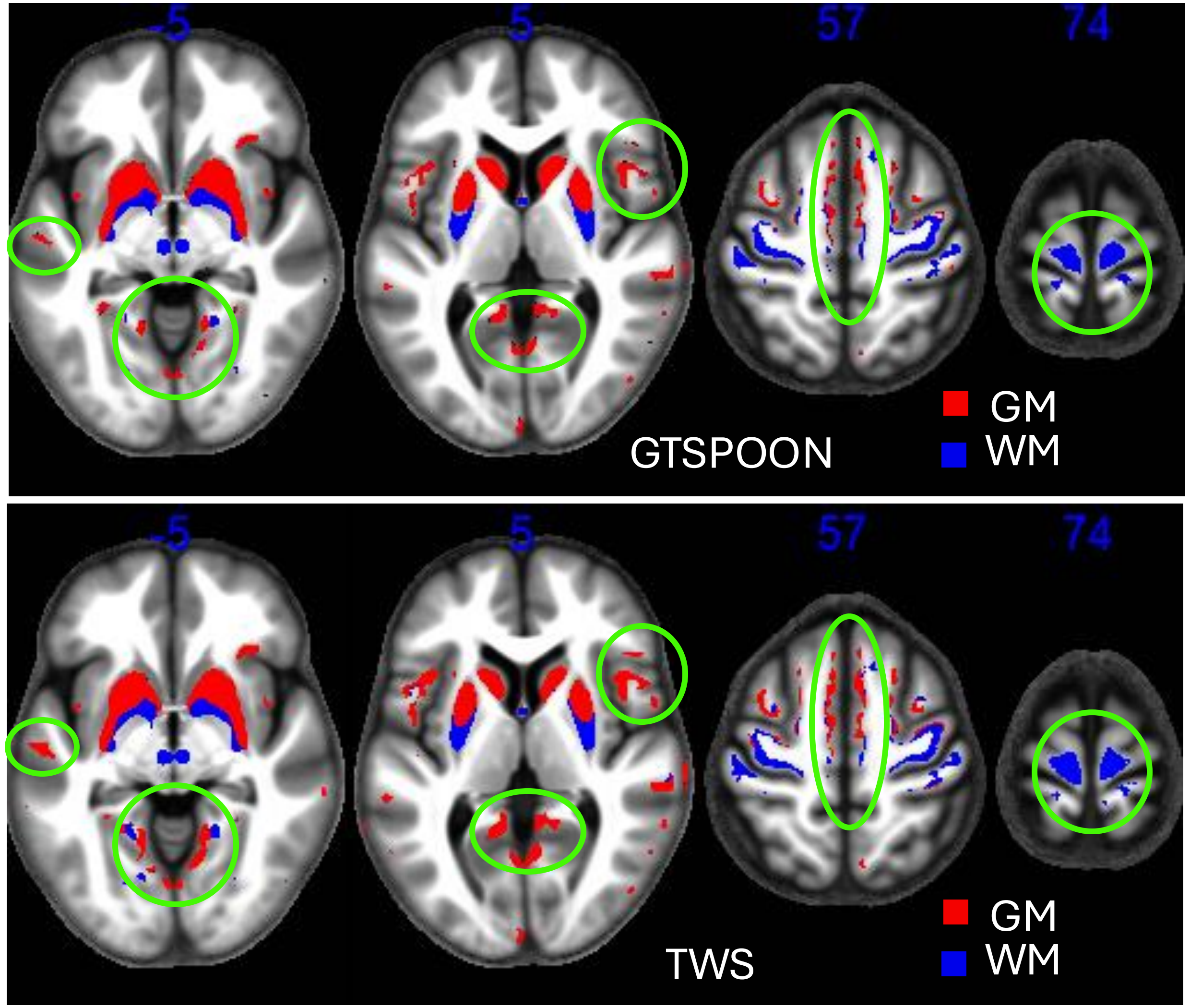

Statistical parametric maps identifying regions in which R2* significantly increase with age

Global trend:

- More significant regions with TWS
- Larger regions with TWS

GM	# Voxels	# Clusters
TWS	41221	659
GTSPOON	34116	512

Consistent with

SPM-based Results

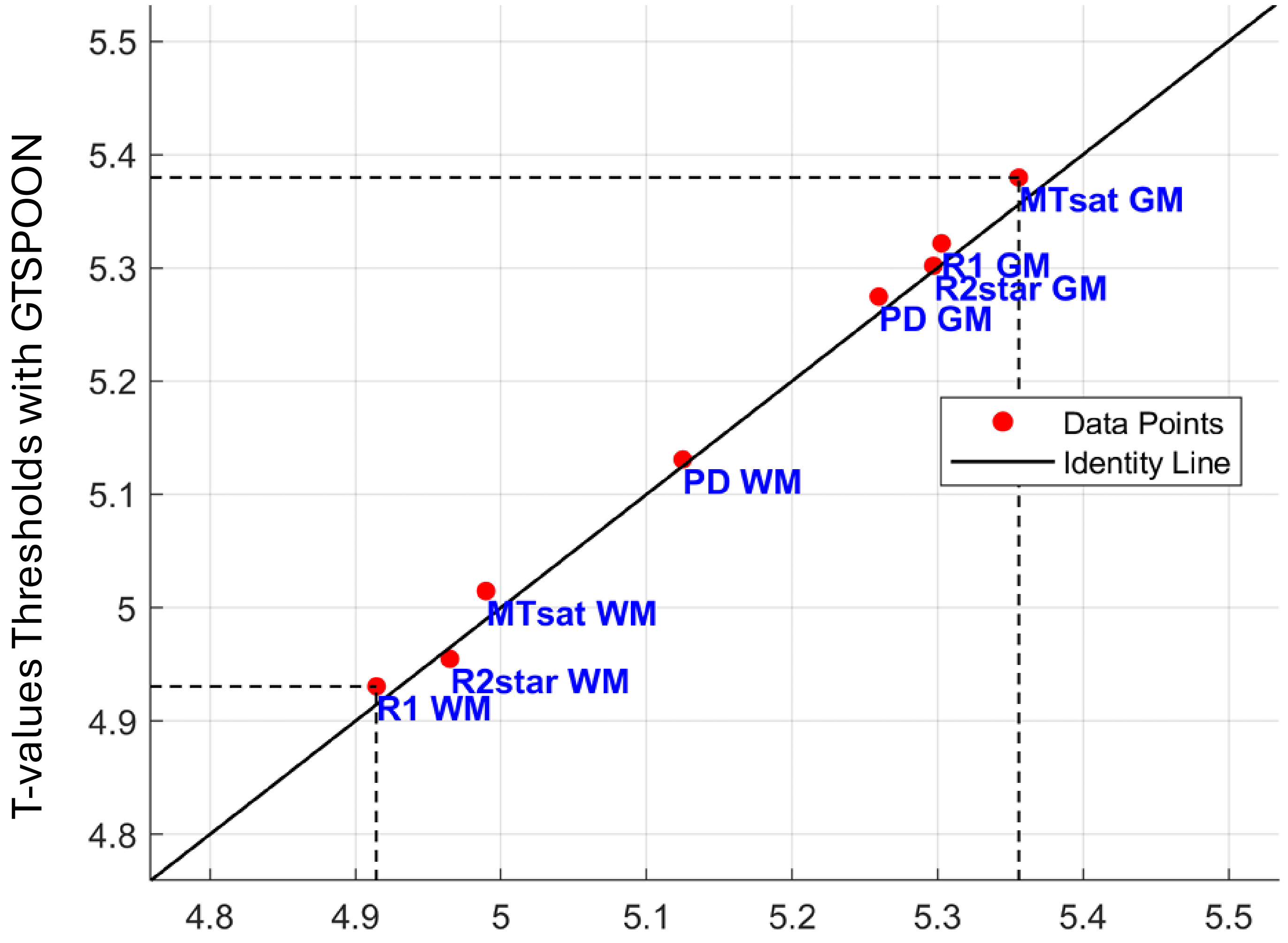

T-values Thresholds with TWS

Thresholds of T-values
($p<0.05$ FWE corrected level)

SPM-based Results

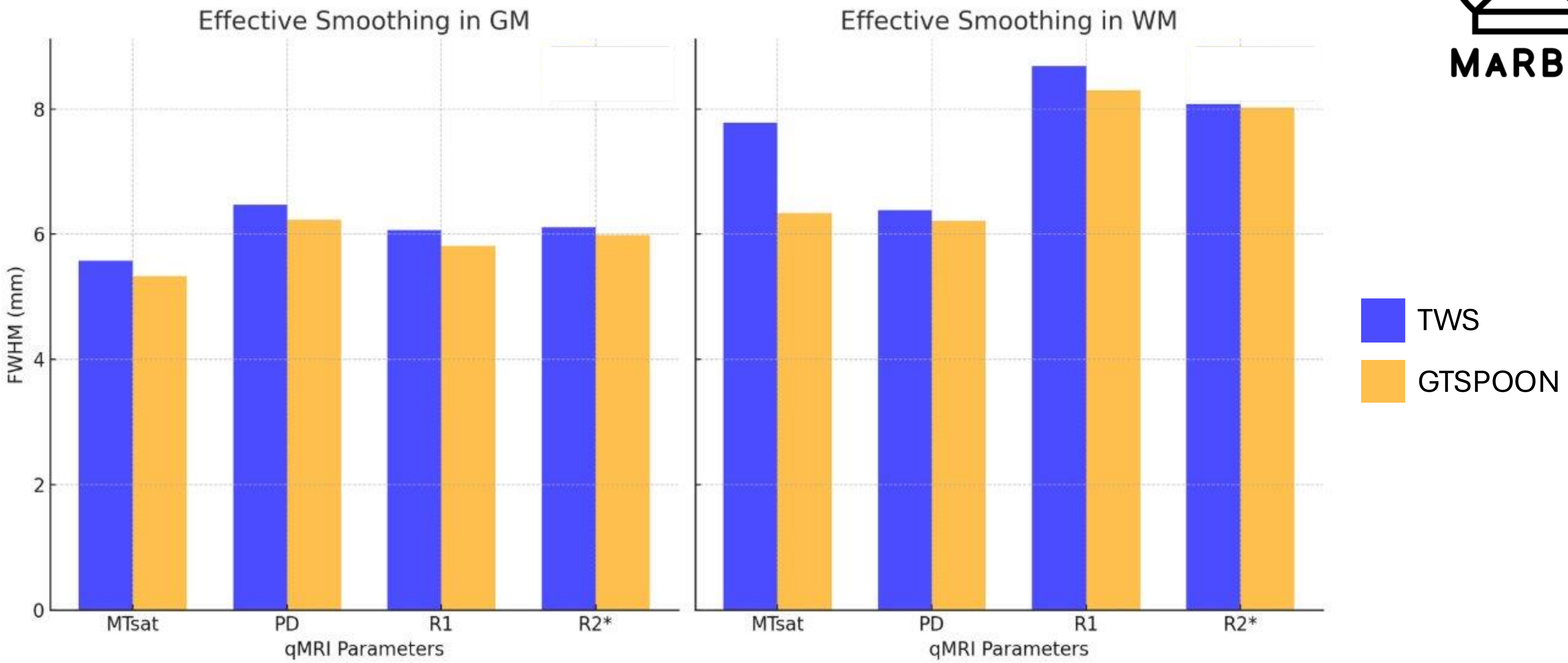

Differences Induced by Smoothing

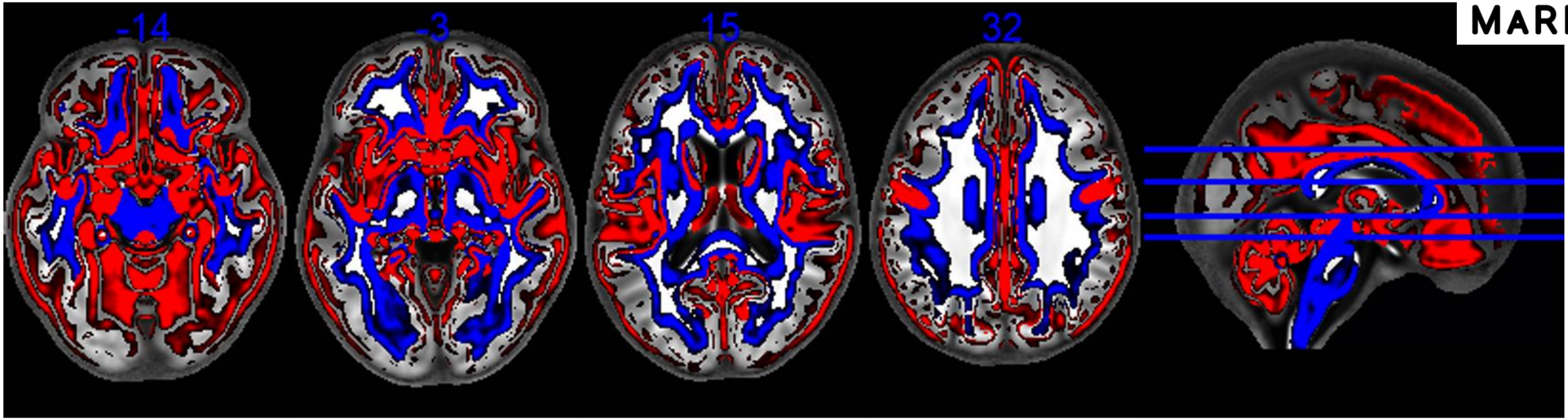

Statistical parametric maps showing regions where Mtsat maps are significantly affected by the subtraction between TWS and GTSPOON at the $p<0.005$ FWE corrected level

GM
WM

Brain 1D Profile

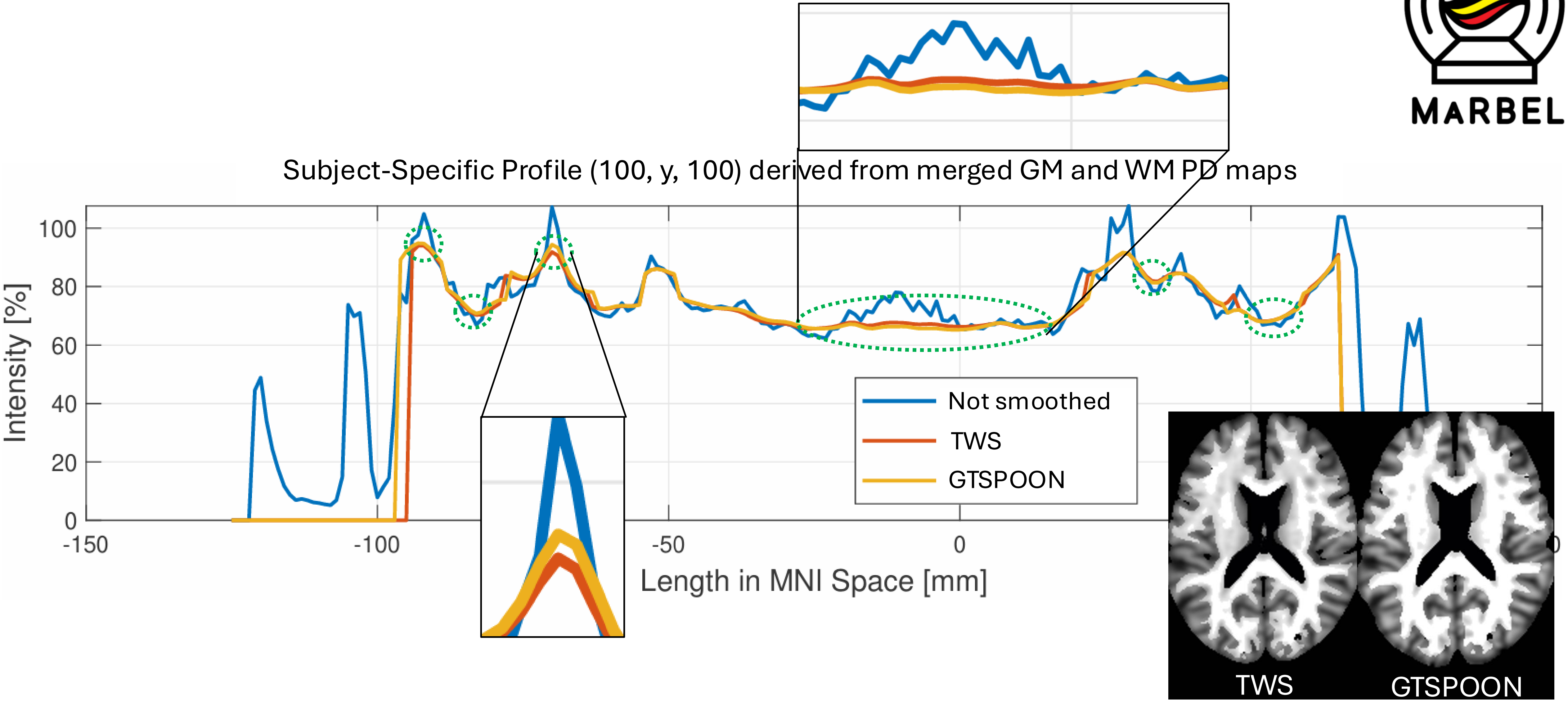

Conclusion & Perspectives

TWS	GTSPOON
Sensitivity	Specificity
Broad signal coverage and detection of subtle variations	Confident and robust detection of localized effects
Longitudinal or population-based studies	Confirmatory and diagnostic studies

- Refining the design of tissue-specific masks
- Extending this smoothing evaluation to diffusion-weighted imaging & positron emission tomography
- Integrating GTSPOON as a new smoothing method in the hMRI toolbox

Reproducibility
Scripts documented on GitHub:
https://github.com/CyclotronResearchCentre/TissueSpecificSmoothing.git

MARBEL

Thank you for your attention!

References

MARBEL

Smoothing Approaches:

- Gaussian Blur. In Wikipedia, 19 novembre 2024. https://en.wikipedia.org/w/index.php?title=Gaussian_blur&oldid=1258405901
- Draganski, B., Ashburner, J., Hutton, C., Kherif, F., Frackowiak, R. S. J., Helms, G., & Weiskopf, N. (2011). Regional specificity of MRI contrast parameter changes in normal ageing revealed by voxel-based quantification (VBQ). NeuroImage, 55(4), 1423-1434. https://doi.org/10.1016/j.neuroimage.2011.01.052
- Lee, J. E., Chung, M. K., Lazar, M., DuBray, M. B., Kim, J., Bigler, E. D., Lainhart, J. E., & Alexander, A. L. (2009). A study of diffusion tensor imaging by tissue-specific, smoothing-compensated voxel-based analysis. NeuroImage, 44(3), 870-883. https://doi.org/10.1016/j.neuroimage.2008.09.041

Datasets:

- Callaghan, M. F., Freund, P., Draganski, B., Anderson, E., Cappelletti, M., Chowdhury, R., Diedrichsen, J., and al. (2014). Widespread age-related differences in the human brain microstructure revealed by quantitative magnetic resonance imaging. Neurobiology of Aging, 35(8), 1862-1872. https://doi.org/10.1016/j.neurobiolaging.2014.02.008

Generalized TSPOON

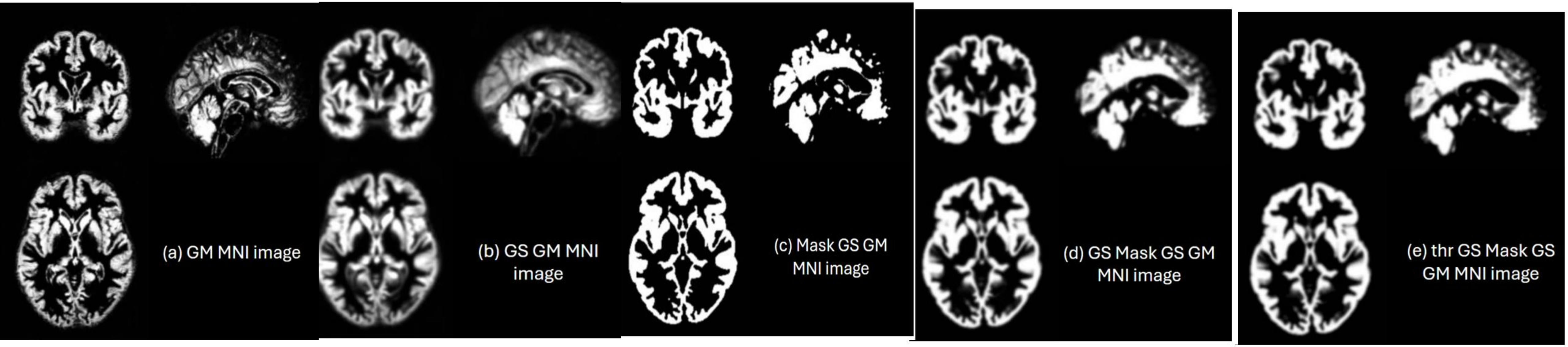

Filling the gaps in the segmentation maps using the **first** Gaussian smoothing

The **second** Gaussian smoothing to mimic the smoothing of the denominator

$$signal_{TC}(x) = \frac{g * (M_{TC}.s(\phi))}{g * M_{TC}} \quad ; \quad g * M_{TC} > 0.05$$

$(M_{TC}.s(\phi)$ **Selection** of a part of the warped quantitative map

The white matter segmentation of DTI images uses the **mFAST** algorithm (FSL toolbox)

In the **core** of the tissue, the values remain equal to 1 while those close to the border are between 0 and 1

Division compensates for the **PVE** induced by the Gaussian smoothing of the selected qMap part

5% threshold to avoid too large multiplicative factor

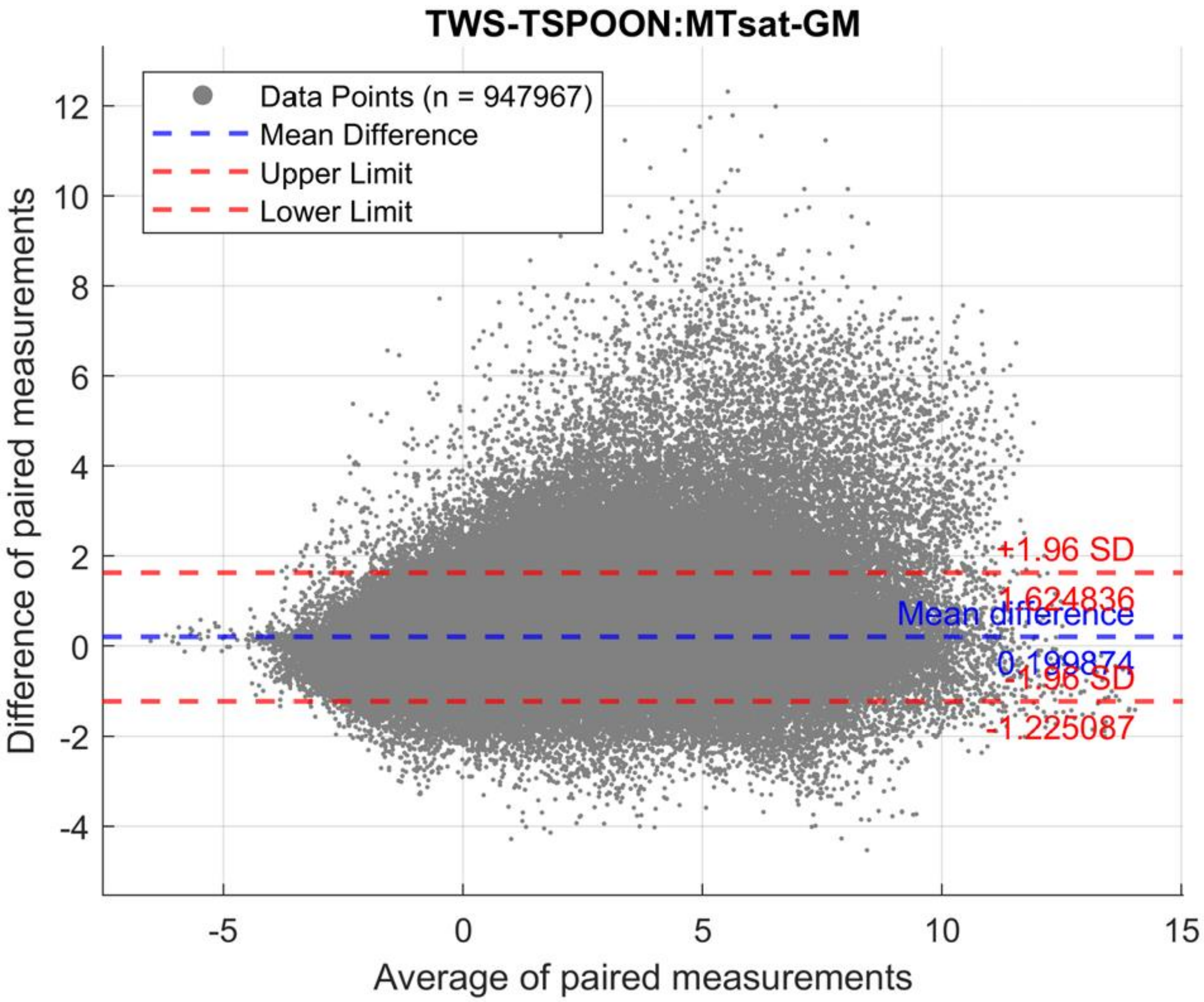

qMRI Parameter	Tissue Class	Jaccard	Dice	Cohen's Kappa
MTsat	GM	0.72222	0.83871	0.83871
	WM	0.63249	0.77488	0.77486
PDmap	GM	0.29595	0.45673	0.45669
	WM	0.89339	0.94369	0.94353
R1map	GM	0.6009	0.7507	0.75063
	WM	0.75472	0.86022	0.86019
R2*map	GM	0.73129	0.84479	0.84397
	WM	0.75579	0.86091	0.86051

Comparison between the TWS and TSPOON methods for AR+.

qMRI Parameter	Tissue Class	Jaccard	Dice	Cohen's Kappa
MTsat	GM	0.59994	0.74995	0.74786
	WM	0.88199	0.9373	0.93666
PDmap	GM	0.69691	0.82139	0.82073
	WM	0.80304	0.89076	0.89033
R1map	GM	0.40337	0.57486	0.57437
	WM	0.81251	0.89656	0.89633
R2*map	GM	0.63973	0.78029	0.78025
	WM	0.83657	0.91101	0.91097

Comparison between the TWS and TSPOON methods for AR-.

Table 4.2: Jaccard index, Dice coefficient and Cohen's kappa between the significant regions ($p < 0.05$ FWE corrected level) derived from the corresponding statistical parameter maps (AR+ and AR-) of TWS and TSPOON for each combination of a qMRI parameter and a tissue class.

Smoothed Quantitative Maps -based qMRI

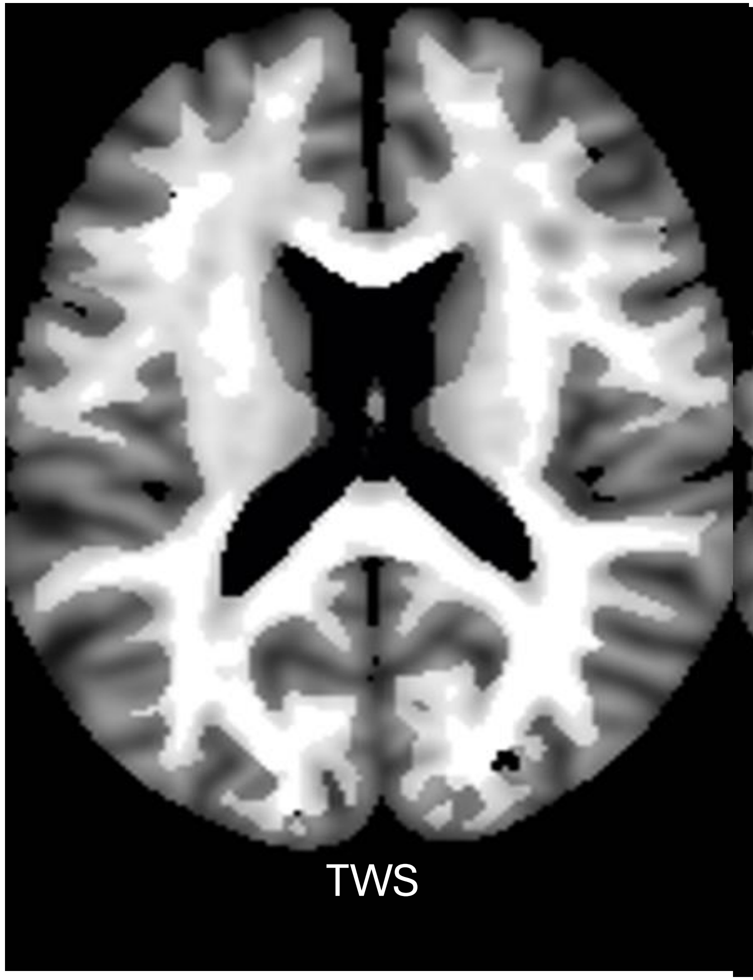

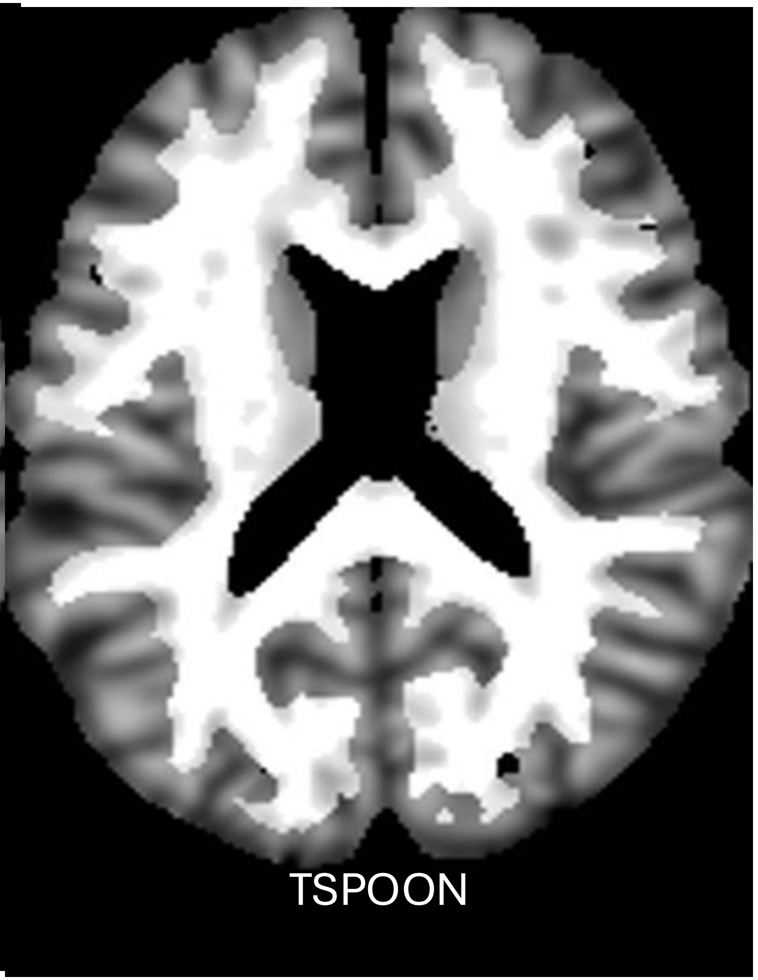

Subject-specific smoothed warped MTsat maps

Discussion

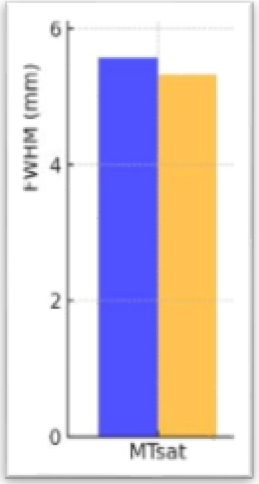

Effective smoothing systematically lower

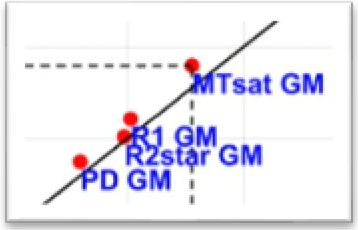

Statistical threshold generally higher

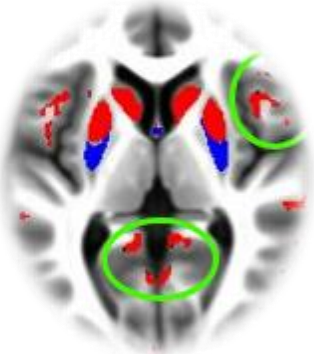

Detection of a greater number of significant clusters and voxels

Differences mainly located at the boundaries between tissues

More sensitive to large variations and less sensitive to small signal variations

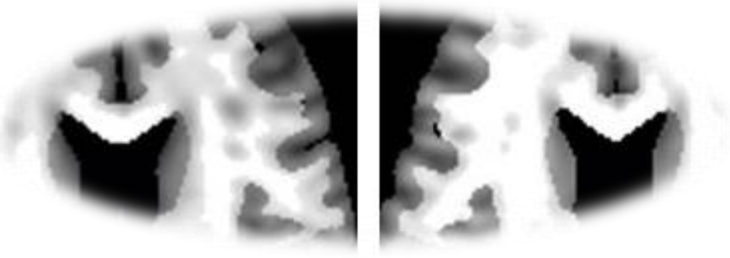

$$\frac{g * (w.s(\phi))}{g * w}$$

Continuous nature of the weights in TWS vs. Binary nature of the optimized mask in TSPOON

$$\frac{g * (M_{TC}.s(\phi))}{g * M_{TC}}$$

Heterogeneity

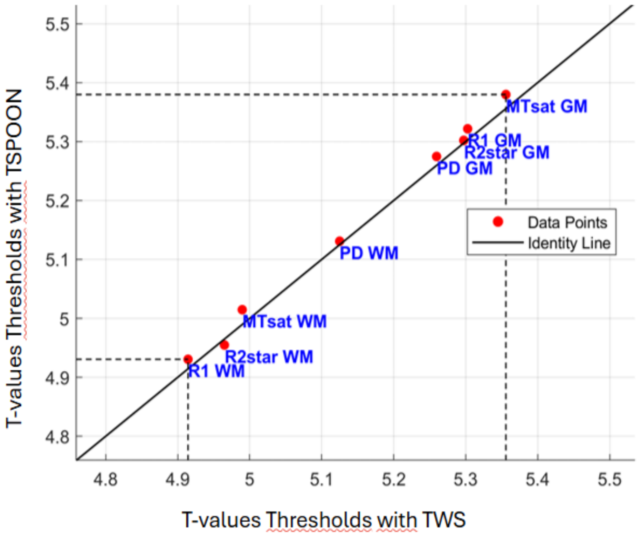

same number of voxels in TWS and TSPOON maps

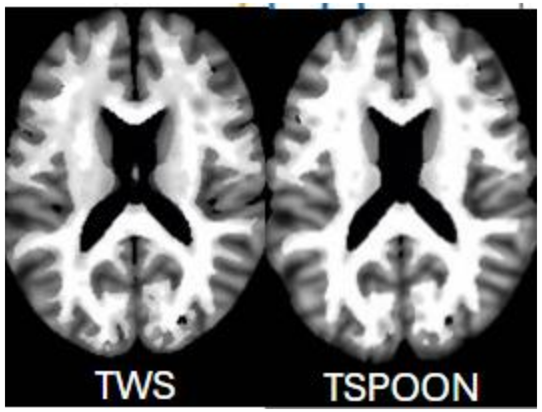

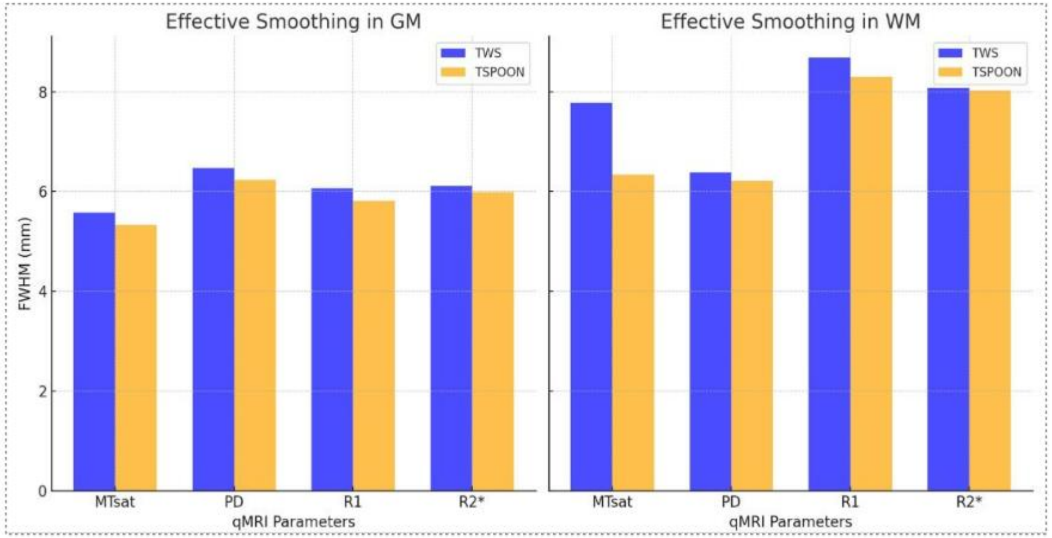

Heterogeneity

Number of resels

measure of the amount of statistically independent information in an image, related to the effective spatial resolution

Number of multiple comparisons

probability of finding a false positive

Statistical threshold